

Lattice QCD study of the strong force among the three quarks

Yoshiaki KOMA*

We present results of the static three-quark potential in quantum chromodynamics obtained by using lattice Monte-Carlo simulations. We investigate the three-quark potential of $O(200)$ sets of the three-quark geometries including not only the cases that three quarks are put at the vertices of acute, right, and obtuse triangles, but also the extreme cases such that three quarks are put in line. We find a clear evidence that the string tension of the three-quark potential is the same as that of the quark-antiquark potential regardless of the geometry of the three quarks.

Key Words: Lattice QCD, Inter-quark potential, Strong force, Baryon

I. INTRODUCTION

Although hadrons such as mesons and baryons are known to be composed of quarks, the underlying structure is not yet completely understood. This is due to difficulty of solving quantum chromodynamics (QCD), a quantum gauge field theory with $SU(3)$ group symmetry, at the energy scale of hadrons where QCD becomes nonperturbative. A possible approach is then to define QCD in four dimensional Euclidean space on a hypercubic discrete lattice and compute the QCD partition function by the Monte-Carlo method (using supercomputers), which is referred to as lattice QCD simulations. This method allows us to compute expectation values of various physical quantities directly without relying on any perturbative techniques.

In this report, we present our recent results of the lattice QCD simulations on the static three-quark potential [1, 2], which is relevant to the understanding of the baryon structure. Our method consists of computing the expectation values of the correlation function of three Polyakov loops (PLCF) at zero temperature accurately by using the noise reduction method called the multilevel algorithm [3, 4], and of extracting the potential from them. We obtain the three-quark potential of $O(200)$ sets of the three-quark geometries including not only the cases that three quarks are put at the vertices of acute, right, and obtuse triangles, but also the extreme cases such that three quarks are put in line. From the derivative of the potential with respect to distances among the three quarks, we find a clear evidence that the string tension of the three-quark potential is the same as that of the quark-antiquark potential regardless of the geometry of the

three quarks. So far, the three-quark potential has been computed by several groups [5–12] by evaluating the expectation value of the three-quark Wilson loop. However, the use of the Wilson loop may cause a systematic effect due to the presence of the junction of spatial Wilson lines, especially when the temporal extent of the Wilson loop is not large enough [13, 14]. It is particularly worth noting that our results are free from such a systematic effect.

II. NUMERICAL PROCEDURES

We consider QCD within the quenched approximation (corresponding to pure $SU(3)$ lattice gauge theory) in four dimensions with the lattice volume $L^3 \times T$ and the lattice spacing a , and impose periodic boundary conditions in all space-time directions. By preparing the three-link correlators, which is a tensor product of the time-like link variables $U_4(x)$ placed at $x = (x_0, \vec{x}_1)$, (x_0, \vec{x}_2) and (x_0, \vec{x}_3) for $x_0 = 0, a, \dots, T - a$,

$$\begin{aligned} & \mathbb{T}(x_0, \vec{x}_{1,2,3})_{\alpha\beta\gamma\delta\epsilon\zeta} \\ & \equiv U_4(x_0, \vec{x}_1)_{\alpha\beta} U_4(x_0, \vec{x}_2)_{\gamma\delta} U_4(x_0, \vec{x}_3)_{\epsilon\zeta}, \end{aligned} \quad (1)$$

where Greek indices take the values from 1 to 3 in $SU(3)$, we construct the three-quark PLCF as

$$\begin{aligned} & \text{Tr}P(\vec{x}_1)\text{Tr}P(\vec{x}_2)\text{Tr}P(\vec{x}_3) \\ & = \{\mathbb{T}(0, \vec{x}_{1,2,3}) \cdots \mathbb{T}(T - a, \vec{x}_{1,2,3})\}_{\alpha\alpha\gamma\gamma\epsilon\epsilon}. \end{aligned} \quad (2)$$

The ground state potential can be extracted from the expectation value of the PLCF with a large T as

$$V_{3q} = -\frac{1}{T} \ln \langle \text{Tr}P(\vec{x}_1)\text{Tr}P(\vec{x}_2)\text{Tr}P(\vec{x}_3) \rangle, \quad (3)$$

where we employ the multilevel algorithm [3, 4]. Note that this algorithm allows us to compute the expectation value accurately even from one gauge configuration [13].

*Division of Liberal Arts / Physics group

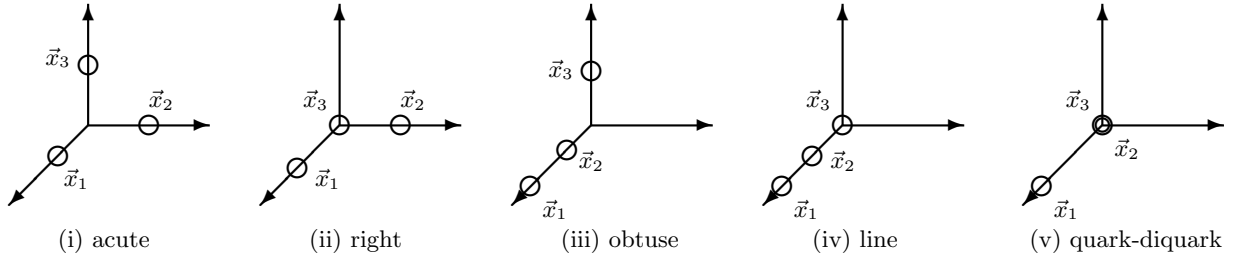


FIG. 1: The three-quark geometries investigated in our numerical simulations. The circles represent the spatial location of quarks. Three Polyakov loops are put at the vertices of (i) acute, (ii) right, (iii) obtuse triangles, and are also put in (iv) line, and are put to be (v) the quark-diquark system.

The spatial locations of the Polyakov loops, \vec{x}_1 , \vec{x}_2 , and \vec{x}_3 correspond to those of three quarks in the three-dimensional space, respectively. There are five types of three-quark geometries: three quarks are put at the vertices of acute (ACT), right (RGT), obtuse (OBT) triangles, and are put in line (LIN) as shown in Fig. 1. As a special case, two of three quarks are put at the same location, which corresponds to a quark-diquark system (QDQ). These three-quark geometries can be classified by the value of the maximum inner angle of a triangle

$$\begin{aligned} \theta_{\max} &= \max(\theta_1, \theta_2, \theta_3) \\ &= \cos^{-1} \left(\frac{r_{\max}(r_1^2 + r_2^2 + r_3^2 - 2r_{\max}^2)}{2r_1 r_2 r_3} \right), \end{aligned} \quad (4)$$

where

$$r_1 = |\vec{x}_2 - \vec{x}_3|, \quad r_2 = |\vec{x}_3 - \vec{x}_1|, \quad r_3 = |\vec{x}_1 - \vec{x}_2|, \quad (5)$$

are interquark distances and $r_{\max} = \max(r_1, r_2, r_3)$. Acute triangles satisfy $\theta_{\max} < 90^\circ$, which contain equilateral and isosceles triangles in our study. Right triangles are the case $\theta_{\max} = 90^\circ$. Obtuse triangles are further classified into two types depending on θ_{\max} , obtuse-narrow (OBTN) triangles for $90^\circ < \theta_{\max} < 120^\circ$ and obtuse-wide (OBTW) triangles for $120^\circ \leq \theta_{\max} < 180^\circ$.

In contrast to the classification of the three-quark geometries, the parametrization of the three-quark potential is not straightforward. This is due to the fact that the potential can depend not only on the location of three quarks, \vec{x}_1 , \vec{x}_2 , and \vec{x}_3 , but also on the structure of the flux tube spanned among the three quarks, which is unknown a priori because of the non-perturbative feature of the QCD vacuum. Therefore,

the determination of the functional form of the potential is nothing but the finding of appropriate distances that can capture the systematic behavior of the potential. Such distances should be symmetric under the permutation of the quark positions.

The simplest distance is then given by the sum of interquark distances in Eq. (5),

$$\Delta = r_1 + r_2 + r_3. \quad (6)$$

Another possible distance is given by the minimal total length of lines connecting the three quarks via the Fermat-Torricelli point of a triangle,

$$Y = \sqrt{\frac{r_1^2 + r_2^2 + r_3^2 + 4\sqrt{3}S}{2}}, \quad (7)$$

where S is the area of the triangle given by Heron's formula,

$$S = \frac{1}{4} \sqrt{\Delta(\Delta - 2r_1)(\Delta - 2r_2)(\Delta - 2r_3)}. \quad (8)$$

Note that the distance between the Fermat-Torricelli point and each vertex is

$$l_i = Y - \frac{1}{Y} \left(r_i^2 + \frac{4S}{\sqrt{3}} \right). \quad (9)$$

Two distances Δ and Y were often used to examine the behavior of the potential in the earlier studies. We also follow them in our analyses of the three-quark potential. In terms of the minimal length of connected lines, Y is reduced to

$$\Lambda = \Delta - r_{\max} \quad (10)$$

when $\theta_{\max} \geq 120^\circ$. It is then convenient to introduce a combined distance of Y and Λ classified by θ_{\max} as

$$L_{\text{str}} = \begin{cases} Y & (\theta_{\max} < 120^\circ) \\ \Lambda & (\theta_{\max} \geq 120^\circ) \end{cases}. \quad (11)$$

III. NUMERICAL RESULTS

We carried out the lattice QCD simulations using the standard Wilson gauge action in SU(3) lattice gauge theory at $\beta = 6.00$ on the 24^4 lattice. The lattice spacing is $a = 0.093$ [fm], determined by the Sommer scale $r_0 = 0.50$ [fm] [15]. One Monte Carlo update consisted of 1 heatbath and 5 over-relaxation steps. The parameters for the multilevel algorithm are $N_{\text{sub}} = 6$ (the number of sublattices), which corresponds to $N_{\text{tsl}} = L/(aN_{\text{sub}}) = 4$, and $N_{\text{iupd}} = 500000$ (the number of internal updates).

Firstly, we focus on the potential of the isosceles triangle geometries within ACT, where the two of three quarks are placed at $\vec{x}_1 = (x, 0, 0)$ and $\vec{x}_2 = (0, x, 0)$, and the remaining third quark is placed at $\vec{x}_3 = (0, 0, z)$ with $z \geq x$. In this case, L_{str} is identical to Y . The distance between the Fermat-Torricelli point and \vec{x}_1 and \vec{x}_2 , respectively, is the same $l_1 = l_2 = (\sqrt{6}/3)x$. Therefore, pulling the third quark (changing z) with the fixed first and second quarks does not affect the location of the Fermat-Torricelli point, which just affects the increase of the energy between the Fermat-Torricelli point and the third quark, where $l_3 = \sqrt{z^2 + x^2/2} - x/\sqrt{6}$. We then compute the derivative of the potential with respect to Y for several fixed values of x ,

$$V'_{3q} = \frac{V_{3q}(x, z + \delta z) - V_{3q}(x, z)}{\delta Y}. \quad (12)$$

In Fig. 2 (upper), we plot the result for one gauge configuration at $\beta = 6.00$ with the classification in terms of the distance between the first and second quarks, $r_{\text{min}} = \sqrt{2}x$, where $x/a = 1, 2$, and 3 (in this case, $\delta Y = \delta l_3$). We find that all the derivatives behave quite similarly and approach a constant value at long distance. Remarkably, the constant value is nothing but the string tension in the quark-antiquark system, $\sigma_{q\bar{q}}a^2 = 0.0449$. Since the third quark is chosen arbitrarily among the three, this result also supports a picture of the Y -shaped flux-tube formation. This feature agrees with that was pointed out by Takahashi *et al.* [9, 10] based on the χ^2 fit to the potential data with the Y Ansatz.

Secondly, we pay attention to the potentials of RGT, where $\vec{x}_2 = (0, y, 0)$ and $\vec{x}_3 = (0, 0, 0)$, and

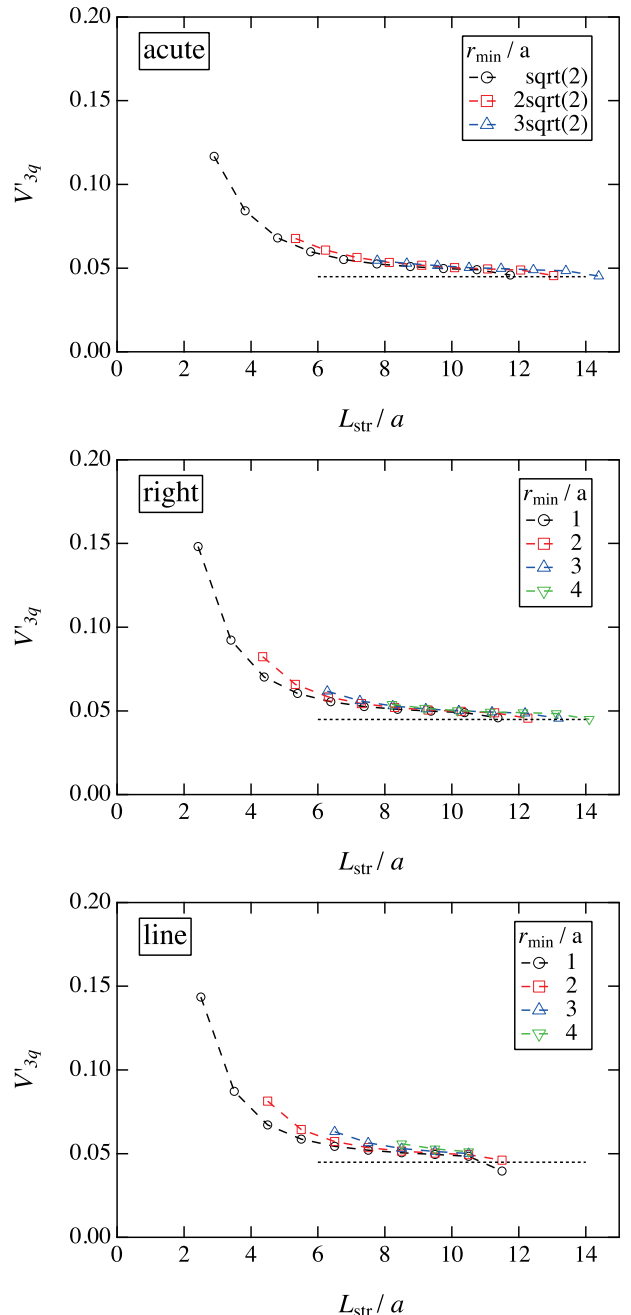


FIG. 2: The derivatives of the three-quark potential with respect to L_{str} for acute (upper), right (middle), and line (lower) geometries. The dotted line in each plot corresponds to the string tension of the quark-antiquark potential $\sigma_{q\bar{q}}a^2 = 0.0449$ [1].

the remaining first quark is placed at $\vec{x}_1 = (x, 0, 0)$ with $x \geq y$. In this case, although the location of the Fermat-Torricelli point is slightly dependent on changing x , it becomes insensitive to x when $x \gg y$. The derivative is then defined by

$$V'_{3q} = \frac{V_{3q}(x + \delta x, y) - V_{3q}(x, y)}{\delta Y}. \quad (13)$$

In Fig. 2 (middle), we plot the result for the same one

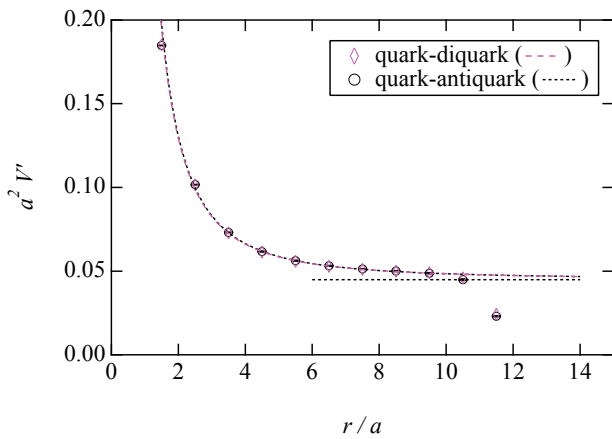


FIG. 3: The derivatives of the quark-diquark and quark-antiquark potentials with respect to r . The horizontal dotted line corresponds to the string tension of the quark-antiquark potential $\sigma_{q\bar{q}}a^2 = 0.0449$ [1].

gauge configuration with the classification in terms of the distance between the second and third quarks, $r_{\min} = y$, where $y/a = 1 \sim 4$. We find that all the derivatives approach the constant value, $\sigma_{q\bar{q}}a^2 = 0.0449$, at long distance: the tendency is quite the same as that for ACT.

Thirdly, we examine the potentials of LIN, where $\vec{x}_1 = (x_1, 0, 0)$, $\vec{x}_2 = (x_2, 0, 0)$, and $\vec{x}_3 = (0, 0, 0)$, which is an extreme case that there is probably no chance to form a junction of the flux tube. For a fixed distance $r_{\min} = x_2$ ($0 < x_2 < x_1/2$), the derivative is then defined by

$$V'_{3q} = \frac{V_{3q}(x_1 + \delta x_1, x_2) - V_{3q}(x_1, x_2)}{\delta x_1}. \quad (14)$$

In Fig. 2 (lower), we plot the result for the same one gauge configuration as a function of $L_{\text{str}} = x_1$. We

again find that all the derivatives approach the constant value, $\sigma_{q\bar{q}}a^2 = 0.0449$, at long distance.

Finally, we look at the quark-diquark system. In Fig. 3, we plot the derivatives of the quark-diquark and quark-antiquark potentials with respect to the interquark distance r . In this case, we find that both data overlap with each other (including finite volume effects at large r), which means that the string tension is exactly the same.

IV. SUMMARY

By using the lattice QCD simulations, we have computed the static three-quark potential of $O(200)$ sets of the three-quark geometries including not only the cases that three quarks are put at the vertices of acute, right, and obtuse triangles, but also the extreme cases such that three quarks are put in line. We have used the PLCF as the three-quark source, which has been quite important to obtain the result with less systematic effect. From the analysis of the derivative of the potential with respect to distances among the three quarks, we have found a clear evidence that the string tension of the three-quark potential is the same as that of the quark-antiquark potential regardless of the geometry of the three quarks.

The author is grateful to M. Koma for fruitful collaboration. The lattice QCD simulations have been performed on the NEC SX8 at Research Center for Nuclear Physics (RCNP), Osaka University. This work is partially supported by JSPS KAKENHI Grant Number 24740176.

-
- [1] Y. Koma and M. Koma, *Phys. Rev.* **D95** (2017) 094513.
[2] Y. Koma and M. Koma, *PoS LAT2015* (2016) 324.
[3] M. Lüscher and P. Weisz, *JHEP* **09** (2001) 010.
[4] M. Lüscher and P. Weisz, *JHEP* **07** (2002) 049.
[5] R. Sommer and J. Wosiek, *Phys.Lett.* **B149**(1984)497.
[6] R. Sommer and J. Wosiek, *Nucl.Phys.***B267**(1986)531.
[7] H. Thacker, E. Eichten, and J. Sexton, *Nucl. Phys. Proc. Suppl.* **4** (1988) 234.
[8] G.S. Bali, *Phys. Rept.* **343** (2001) 1.
[9] T.T. Takahashi, H. Matsufuru, Y. Nemoto, and H. Suganuma, *Phys. Rev. Lett.* **86** (2001) 18.
[10] T.T. Takahashi, H. Suganuma, Y. Nemoto, and H. Matsufuru, *Phys. Rev.* **D65** (2002) 114509.
[11] C. Alexandrou, Ph. de Forcrand, and A. Tsapalis, *Phys. Rev.* **D65** (2002) 054503.
[12] F. Bissey, F.G. Cao, A.R. Kitson, A.I. Signal, D.B. Leinweber, B.G. Lasscock, and A.G. Williams, *Phys. Rev.* **D76** (2007) 114512.
[13] Y. Koma and M. Koma, *PoS LAT2013* (2013) 469.
[14] Y. Koma and M. Koma, *PoS LAT2014* (2014) 352.
[15] S. Necco and R. Sommer, *Nucl. Phys.* **B622** (2002) 328.